Chapter 2
Modeling of Open Channel Flow

Abstract In this chapter, we present the classical model used to describe open channel hydraulics: the Saint-Venant equations. For completeness, the equations are rigorously derived in Appendix A. We first study some of their mathematical properties, such as the characteristic form. We briefly describe some numerical methods of resolution, and then consider the linearized equations that are valid for small variations around equilibrium regimes. These equations form the basis of all the methods developed in this book.

2.1 Saint-Venant Equations for Open Channel Flow

The Saint-Venant equations were first stated in 1871 in a note to the Comptes-Rendus de l'Académie des Sciences de Paris by Adhémar Barré de Saint-Venant, a French engineer of Ponts et Chaussées [15]. This has remained one of the most popular models among hydraulic engineers to represent the dynamics of open channel flow. It has been applied successfully in many applications, such as river flow forecasting, canal operations, sewer modeling, etc. (see the book by Cunge et al. [6], which is a classical reference for hydraulic engineers).

2.1.1 Saint-Venant Equations

In this section we give the Saint-Venant equations, which express the conservation of mass and momentum for one-dimensional open channel flow. Before stating the equations, we give the hypotheses used in their derivation, and define the notations. The derivation of the equations is detailed in Appendix A for completeness.

2.1.1.1 Hypotheses and Notations

The following assumptions are classically made when deriving the Saint-Venant equations:

1. The flow is one-dimensional, i.e., the velocity is uniform over the cross-section and the water level across the section is horizontal.
2. The streamline curvature is small and vertical accelerations are negligible, hence the pressure is hydrostatic.
3. The effect of boundary friction and turbulence can be accounted for through resistance laws analogous to those used for steady-state flow.
4. The average channel bed slope is small so that the cosine of the angle it makes with the horizontal may be replaced by unity.
5. The variation of channel width along x is small.

We denote by x the longitudinal abscissa and by t the time. We shall use the following notations for the considered variables (see Figs. 2.1 and 2.2): $A(x,t)$ represents the wetted area (m^2), $Q(x,t)$ the discharge (m^3/s) across-section A, $V(x,t)$ the average velocity (m/s) in section A, $Y(x,t)$ the water depth (m), $S_f(x,t)$ the friction slope (m/m), $S_b(x)$ the bed slope (m/m), and g the gravitational acceleration (m/s^2).

We assume that the distributed lateral inflow and outflow are negligible. The methods developed in the book may be readily extended to the case of nonzero lateral inflow or outflow.

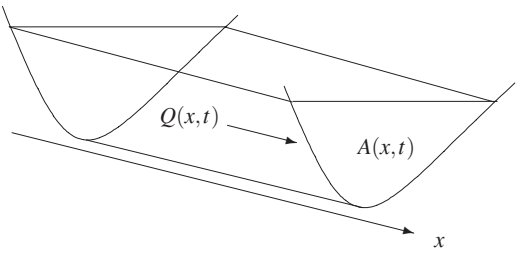

Fig. 2.1 Open channel flow along a longitudinal axis indexed by the abscissa x. The discharge $Q(x,t)$ is defined as $Q(x,t) = A(x,t)V(x,t)$

2.1.1.2 The Equations

The Saint-Venant equations are two coupled partial derivative equations. The first one is the mass conservation equation:

$$\frac{\partial A(x,t)}{\partial t} + \frac{\partial Q(x,t)}{\partial x} = 0, \tag{2.1}$$

and the second one is the momentum conservation equation:

$$\frac{\partial Q(x,t)}{\partial t} + \frac{\partial}{\partial x}\left[\frac{Q^2(x,t)}{A(x,t)}\right] + gA(x,t)\left(\frac{\partial Y(x,t)}{\partial x} + S_f(x,t) - S_b(x)\right) = 0. \tag{2.2}$$

The friction slope S_f is modeled with the classical Manning formula [5]:

$$S_f = \frac{Q^2 n^2}{A^2 R^{4/3}}, \tag{2.3}$$

with n the Manning coefficient ($\mathrm{sm}^{-1/3}$) and R the hydraulic radius (m), defined by $R = A/P$, where P is the wetted perimeter (m) (see Fig. 2.2).

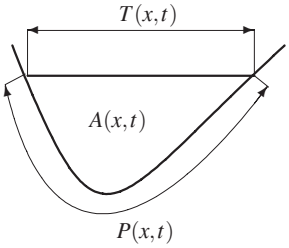

Fig. 2.2 Section of an open channel. Definition of the wetted perimeter P, wetted area A, and top width T

2.1.1.3 Initial and Boundary Conditions

To complete the equations, we need to introduce initial and boundary conditions.

The initial condition is given in terms of $(Q(x,0), Y(x,0))$, for all $x \in [0, L]$, with L the length of the channel.

The choice of the boundary conditions depends on the flow characteristics, and the reverse also holds, since a change in the boundary conditions may change the flow characteristics. This choice will be discussed in Sect. 2.1.4, once the characteristic form of the equations has been introduced.

2.1.1.4 Available Measurements and Controls

Since our objective is to control open channel flow using boundary controls, we need to specify the measurements and controls available. In many practical situations, the available controls are gate openings, and the available measurements are boundary water levels. However, for reasons that will be clarified later, we will consider that we can control the boundary discharges $Q(0,t)$ and $Q(L,t)$, and that we measure the

boundary water depths $Y(0,t)$ and $Y(L,t)$. More generally, one may measure water levels at various locations along the canal, but for practical reasons, the boundary levels are easier to measure.

2.1.2 Limitations of Saint-Venant Equations

The Saint-Venant equations are valid as long as the hypotheses stated in Sect. 2.1.1.1 are fulfilled. We mention here some cases where these hypotheses do not hold.

2.1.2.1 Two-dimensional Flow

When the flow is not one-dimensional, which may happen in flood plains or in large rivers, the one-dimensional Saint-Venant equations are inaccurate. In that case, one may consider two-dimensional Saint-Venant equations. We restrict ourselves in this book to flow patterns that can reasonably be modeled with a one-dimensional flow assumption. This is the case of most of open channels that are controlled with hydraulic structures: irrigation or drainage canals, regulated rivers, and sewers.

2.1.2.2 Non-hydrostatic Pressure Distribution

When the pressure distribution is not hydrostatic, the pressure term in the Saint-Venant equations needs to be modified. This is usually linked to hydraulic phenomenon with a small wave length, either due to geometric variations (sharp bend) or hydraulic variations, e.g., undular hydraulic jump, or undular tidal bore.

In this case, a more accurate model is provided by the Boussinesq equations. These equations add a third order derivative term to the momentum conservation of the Saint-Venant equations [21]. Undular bores are positive surges characterized by a train of secondary waves following the surge front. They were studied originally by Favre [8] and are efficiently modeled with the Boussinesq equations [4, 18, 13].

2.1.2.3 Sharp Discontinuities

When the flow encounters sharp discontinuities, such as those provoked by hydraulic structures (weirs or gates), the Saint-Venant equations are no longer applicable. These hydraulic structures are usually treated as internal boundaries modeled with a static algebraic relationship between the flow variables. This static relationship is usually derived from the Bernoulli theorem. In this book, we consider hydraulic structures as passive static controllers acting at the boundaries of the domain. This point will be developed in Chap. 6.

2.1.3 Characteristic Form

The Saint-Venant equations are nonlinear hyperbolic partial differential equations, that can be expressed as a set of four ordinary differential equations in the (x,t) plane using the classical "characteristic form" [1]. These ordinary differential equations are satisfied along the so-called "characteristic curves" in the (x,t) plane. The characteristic form is important because it has long been used as a classical means to solve the equations in simple cases, and because it enables us to understand the physical phenomenon modeled by the hyperbolic equations.

For simplicity, in the following we consider a rectangular prismatic channel, i.e., a channel with a spatially uniform rectangular cross-section.

We first rewrite the equations in terms of the velocity V and the water depth Y. Let T denote the top width (see Fig. 2.2). The area is then equal to $A(x,t) = TY(x,t)$, and the continuity equation then reads:

$$\frac{\partial Y}{\partial t}(x,t) + Y(x,t)\frac{\partial V}{\partial x}(x,t) + V(x,t)\frac{\partial Y}{\partial x}(x,t) = 0. \tag{2.4}$$

For the momentum equation, we first replace $Q(x,t) = TY(x,t)V(x,t)$ in (2.2), apply the product rule of differentiation, and substitute for $\frac{\partial Y}{\partial t}(x,t)$ from the continuity equation (2.4). Finally, dividing by $A(x,t)$ leads to:

$$\frac{\partial V}{\partial t}(x,t) + V(x,t)\frac{\partial V}{\partial x}(x,t) + g\frac{\partial Y}{\partial x}(x,t) = g(S_b - S_f(x,t)). \tag{2.5}$$

Let us introduce the variable $C(x,t) = \sqrt{g\frac{A(x,t)}{T(x,t)}}$ (here $C(x,t) = \sqrt{gY(x,t)}$ due to the rectangular geometry), which is homogeneous to a celerity.

We now express (2.5–2.4) in terms of variables $V(x,t)$ and $C(x,t)$. Using the fact that $\frac{\partial C}{\partial t} = \frac{g}{2C}\frac{\partial Y}{\partial t}$, and dropping the dependence in (x,t) for readability, we get:

$$2\frac{\partial C}{\partial t} + C\frac{\partial V}{\partial x} + 2V\frac{\partial C}{\partial x} = 0, \tag{2.6a}$$

$$\frac{\partial V}{\partial t} + V\frac{\partial V}{\partial x} + 2C\frac{\partial C}{\partial x} = g(S_b - S_f). \tag{2.6b}$$

Now, we observe that adding and subtracting (2.6a) and (2.6b) respectively leads to:

$$\frac{\partial}{\partial t}(V + 2C) + (V + C)\frac{\partial}{\partial x}(V + 2C) = g(S_b - S_f), \tag{2.7a}$$

$$\frac{\partial}{\partial t}(V - 2C) + (V - C)\frac{\partial}{\partial x}(V - 2C) = g(S_b - S_f). \tag{2.7b}$$

We have obtained a set of equations with two new variables

$$J_1(x,t) = V(x,t) + 2C(x,t),$$
$$J_2(x,t) = V(x,t) - 2C(x,t).$$

Then, we remark that the left-hand terms of (2.7) involve a derivative along two characteristic curves. A characteristic curve is defined in the (x,t) plane by an ordinary differential equation such as:

$$\frac{\mathrm{d}x}{\mathrm{d}t} = U(x(t),t). \tag{2.8}$$

This can be depicted as in Fig. 2.3. A characteristic curve described by (2.8) has a local slope equal to $1/U(x_M,t_M)$ at the point of coordinates (x_M,t_M).

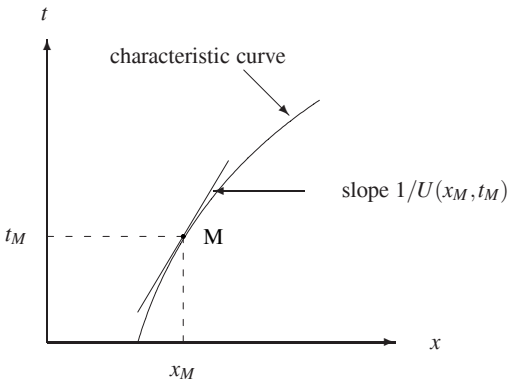

Fig. 2.3 Characteristic line $\frac{\mathrm{d}x}{\mathrm{d}t} = U(x(t),t)$ in the (x,t) plane

Then, the time derivative of a variable $Z(x(t),t)$ along a characteristic curve defined by (2.8) is given by:

$$\frac{\mathrm{d}Z}{\mathrm{d}t}(x(t),t) = \frac{\partial Z}{\partial t}(x(t),t) + U(x(t),t)\frac{\partial Z}{\partial x}(x(t),t). \tag{2.9}$$

Applying this property to (2.7), we obtain the following expressions:

$$\frac{\mathrm{d}J_1}{\mathrm{d}t}(x_1,t) = h(x_1,J_1(x_1,t),J_2(x_1,t)), \tag{2.10a}$$

$$\frac{\mathrm{d}x_1}{\mathrm{d}t} = V(x_1,t)+C(x_1,t), \tag{2.10b}$$

$$\frac{\mathrm{d}J_2}{\mathrm{d}t}(x_2,t) = h(x_2,J_1(x_2,t),J_2(x_2,t)), \tag{2.10c}$$

$$\frac{\mathrm{d}x_2}{\mathrm{d}t} = V(x_2,t)-C(x_2,t), \tag{2.10d}$$

with $h(x,J_1(x,t),J_2(x,t)) = g(S_b(x)-S_f(x,J_1(x,t),J_2(x,t)))$, and where the dependence of $x_1(t)$ and $x_2(t)$ on t has been dropped for readability.

The four ordinary differential equations (2.10) are then equivalent to the Saint-Venant equations.

2.1.3.1 Supercritical Versus Subcritical Flow

Such a characteristic form is in fact a very general feature of hyperbolic partial differential equations [7]. It is also useful to understand the fundamental physical behavior of open channel flow: the discharge and water depth (or, equivalently, the velocity and the area) are the result of the interaction of two elementary waves, one traveling downstream, corresponding to the positive characteristic curve C_1, the other one traveling either upstream or downstream, depending on the sign of $V-C$, corresponding to the negative characteristic curve C_2. When $V < C$, the negative characteristic curve C_2 travels upstream, and the flow is called subcritical. When $V > C$, the negative characteristic C_2 curve travels downstream, and the flow is called supercritical (see Fig. 2.4).

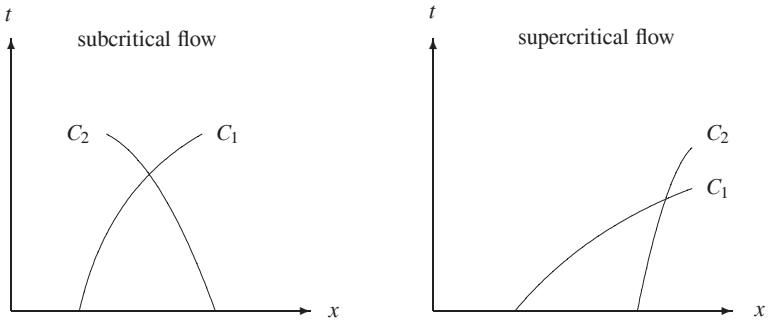

Fig. 2.4 Characteristics in subcritical and supercritical flow

For illustration purposes, we consider below the horizontal frictionless case to give a physical interpretation of these expressions.

2.1.3.2 Horizontal Frictionless Case

In the special case of a horizontal frictionless channel, the slope S_b and the friction slope S_f are identically zero, so that the function $h(x,J_1(x,t),J_2(x,t)) \equiv 0$, which leads to:

$$\frac{\mathrm{d}J_1}{\mathrm{d}t}(x_1,t) = 0 \tag{2.11a}$$

$$\frac{\mathrm{d}x_1}{\mathrm{d}t} = V(x_1,t) + C(x_1,t) \tag{2.11b}$$

$$\frac{\mathrm{d}J_2}{\mathrm{d}t}(x_2,t) = 0 \tag{2.11c}$$

$$\frac{\mathrm{d}x_2}{\mathrm{d}t} = V(x_2,t) - C(x_2,t). \tag{2.11d}$$

In this case, (2.11) can be interpreted as follows:

- The total derivative of the quantity $J_1 = V + 2C$ is zero along the characteristic curve defined by (2.11b). Therefore, this quantity conserves its initial value along the first characteristic curve. This can be displayed in the (x,t) plane, where the solution of (2.11b) is a line denoted C_1, with a positive slope equal to $1/(V+C)$. This corresponds to a wave traveling downstream.
- Similarly, the total derivative of the quantity $J_2 = V - 2C$ is zero along the characteristic curve defined by (2.11d). Therefore, this quantity conserves its initial value along the second characteristic curve. In the (x,t) plane, the solution of (2.11d) is a line denoted C_2, with a slope equal to $1/(V-C)$, which may be negative or positive. When $V > C$, this wave is traveling downstream, otherwise it is traveling upstream.

Therefore, in the horizontal frictionless case, the variables $J_1(x,t)$ and $J_2(x,t)$ are constant along the characteristic curves C_1 and C_2. J_1 and J_2 are called *Riemann invariants* of the hyperbolic system.

In this case, the characteristics method provides a way to derive an analytical solution to the Saint-Venant equations for simple initial conditions. This point will be detailed in Sect. 2.4.2 for the linearized equations, which apply for small variations of depth and discharge around a steady flow.

2.1.3.3 General Case

In the general case, the right-hand term $h(x,J_1(x,t),J_2(x,t))$ is different from zero, and $J_1(x,t)$ and $J_2(x,t)$ are called quasi-invariants, since their values change along the characteristics lines. There is no analytical solution in that case, but the charac-

teristic form can be used to solve the equations numerically. Some classical numerical methods will be presented in Sect. 2.2.

The characteristic form displayed in (2.10) is valid only for rectangular prismatic geometry, but can be generalized to more complex geometry. The expressions of the quasi-invariants are more complex, but they keep the same physical meaning: the flow can be described as the interaction of two waves in the plane (x,t), one that travels at speed $V+C$, the another that travels at speed $V-C$.

2.1.4 *Influence of Initial and Boundary Conditions*

The characteristics enable us to understand the way an initial condition propagates in the domain. The initial condition will have a range of influence in a triangularly shaped domain in the (x,t) plane (see Fig. 2.5). For the rest of the (x,t) plane, one needs to specify the boundary conditions at $x=0$ and $x=L$.

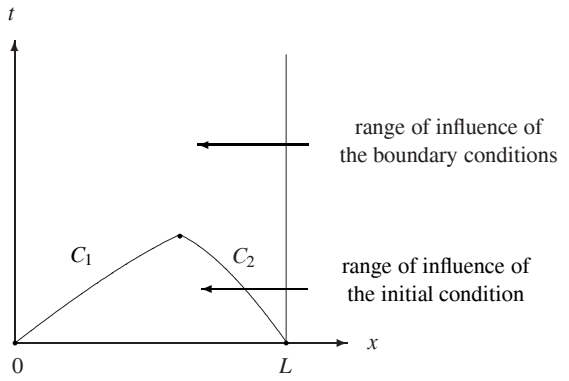

Fig. 2.5 Range of influence of the initial and boundary conditions for subcritical flow

As mentioned above, it is possible to define different boundary conditions according to the flow characteristics. The characteristic form of the equations is useful for understanding the different possible boundary conditions that one may define:

- If the flow is subcritical, two boundary conditions are needed, one upstream and one downstream.
- If the flow is supercritical, two boundary conditions must be defined at the upstream boundary.
- For intermediate situations, i.e., when the flow in the channel is partly subcritical and partly supercritical, one may need to specify one, two, or three boundary

conditions according to the situation. One possibility is then to deal with weak boundary conditions [3, 19]. This complex situation is out of the scope of this book.

We will assume in the rest of the book that the flow is subcritical over the whole channel; therefore we need one condition at each boundary (see Fig. 2.6).

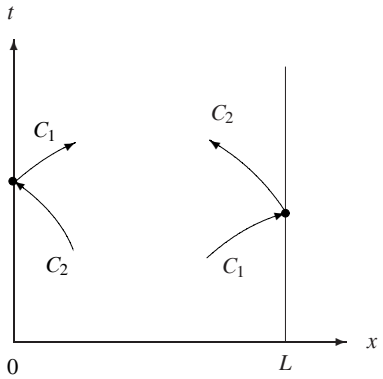

Fig. 2.6 Boundary conditions for subcritical flow

We can either choose the water depth or the discharge as a boundary condition. There are therefore four possibilities:

1. Discharges at both boundaries: $(Q(0,t),Q(L,t))$. This corresponds to the case where two pumps impose the discharges at each boundary, where the canal is closed. This is the case that we will mostly consider in this book, since we will assume that a hydraulic structure such as a gate can deliver a given discharge.
2. Water depths at both boundaries: $(Y(0,t),Y(L,t))$. This corresponds to the case of a body of water connected at each end to very large bodies of water. Such a situation can occur in deltaic zones, where a river can be connected to the sea at one end, and to a lake at the other end.
3. Discharge upstream and water depth downstream: $(Q(0,t),Y(L,t))$. This case corresponds to the case of a river where the upstream discharge is controlled by a dam, and the downstream ends up in a lake.
4. Water upstream and discharge downstream: $(Y(0,t),Q(L,t))$. This unusual case may correspond to a hydroelectric power plant controlling the downstream discharge of a river leaving from a lake.

The developments of this book mainly consider the first case, but can be adapted to the other cases without much difficulty.

2.1.5 Calibration of the Saint-Venant Model

When faced with a practical problem of modeling an open channel, a hydraulic engineer usually requires the following data:

- Physical parameters describing the geometry of the open channel: slope, cross-section (shape, dimension, and variation along x).
- Value of the Manning friction coefficient.

Usually, the geometry can be obtained with a measuring campaign, and the Manning coefficient can be either estimated from tables, or calibrated based on steady-state water level and discharge measurements.

2.2 Numerical Methods of Resolution

While this book is not aimed at providing state of the art numerical methods of resolution, for completeness we briefly mention two classical numerical methods of resolution, the method of characteristics and the finite difference Preissmann scheme.

2.2.1 The Method of Characteristics

We present two numerical methods based on the characteristics: the original method and the Hartree method.

2.2.1.1 The Original Method

The characteristic form of the Saint-Venant equations that we derived in Sect. 2.1.3 can be used to numerically solve the equations. This method has been detailed extensively by Abbott [1, 2]. In the following we give an illustration of the method in the rectangular case. Let us assume that initial data are known at points A and B (see Fig. 2.7).

The characteristics issuing from these points intersect at the point C. Equations (2.10) can be integrated along the characteristics as follows:

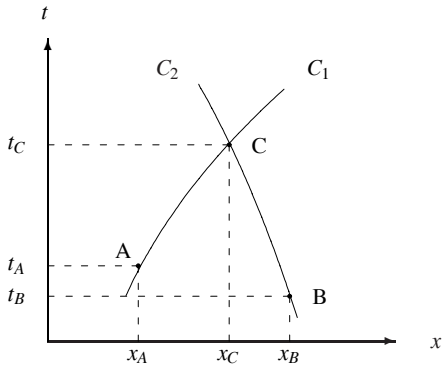

Fig. 2.7 Numerical resolution with the method of characteristics

$$V_C + 2C_C = V_A + 2C_A + \int_{t_A}^{t_C} g(S_b - S_f)\mathrm{d}t \tag{2.12a}$$

$$x_C = x_A + \int_{t_A}^{t_C} (V + C)\mathrm{d}t \tag{2.12b}$$

$$V_C - 2C_C = V_B - 2C_B + \int_{t_B}^{t_C} g(S_b - S_f)\mathrm{d}t \tag{2.12c}$$

$$x_C = x_B + \int_{t_B}^{t_C} (V - C)\mathrm{d}t. \tag{2.12d}$$

These four equations can be solved for the unknowns V_C, C_C, x_C, and t_C. To this end, one needs to evaluate the integral terms. A classical approximation is to use the trapezoidal rule of integration between points A and C, and between points B and C.

The method of characteristics provides an elegant way to turn the two nonlinear partial differential equations (PDE) into a set of four nonlinear ordinary differential equations (ODE), which may be solved numerically. However, the solution is obtained on an irregular grid, which consists of the points of the (x,t) plane located at the intersection of two characteristics: a forward characteristic and a backward characteristic. This requires us to perform an interpolation in order to compute the flow variables at fixed locations.

2.2.1.2 The Hartree Method

The Hartree method enables to use the characteristics method with a fixed grid in the (x,t) plane. Let us assume that the flow properties are known at time $t = (k-1)\Delta t$, and that we want to compute the flow at point $\mathrm{C}(x_C, k\Delta t)$. The idea is to compute

the characteristics backwards in time and to interpolate the solution at time t (see Fig. 2.8).

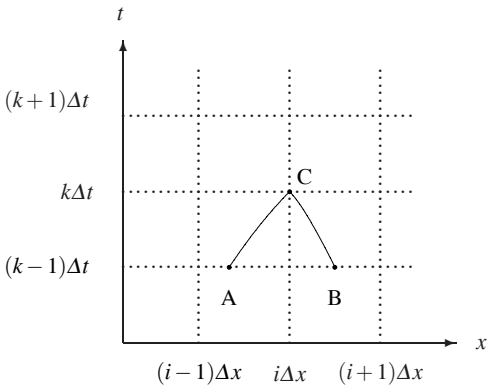

Fig. 2.8 Numerical resolution with the Hartree method

The abscissa of points A and B do not generally coincide with the fixed grid points. It is then necessary to interpolate the velocity and celerity at points A and B between $x = (i-1)\Delta x$ and $x = i\Delta x$, and between $x = i\Delta x$ and $x = (i+1)\Delta x$, respectively. The corresponding discrete characteristic equations are given by:

$$V_C + 2C_C = V_A + 2C_A + g(S_b - S_{fA})\Delta t, \tag{2.13a}$$

$$x_C - x_A = (V_A + C_A)\Delta t, \tag{2.13b}$$

$$V_C - 2C_C = V_B - 2C_B + g(S_b - S_{fB})\Delta t, \tag{2.13c}$$

$$x_C - x_B = (V_B - C_B)\Delta t. \tag{2.13d}$$

The resulting system has four unknowns, V_C, C_C, x_A, and x_B, where the subscripts refer to the points A, B, and C in Fig. 2.8.

The system (2.13) can be solved explicitly using a linear interpolation for the values of V and C at points A and B.

The method of characteristics is an explicit method, which is subject to the Courant–Friedrichs–Levy stability condition:

$$\Delta t < \frac{\Delta x}{|V \pm C|}. \tag{2.14}$$

Therefore, according to the defined space step of the considered problem, the time step size is limited by this condition. This may lead to large computation times.

2.2.2 The Preissmann Implicit Scheme

This implicit scheme was first proposed by Alexandre Preissmann in 1961 when he was hydraulic engineer at SOGREAH, Grenoble, France [14]. In the general Preissmann scheme, a continuous function $f(x,t)$ and its partial derivatives are represented by [6, 22]:

$$f(x,t) = \theta\left[\phi f_{i+1}^{k+1} + (1-\phi) f_i^{k+1}\right] + (1-\theta)\left[\phi f_{i+1}^{k} + (1-\phi) f_i^{k}\right], \tag{2.15a}$$

$$\frac{\partial f}{\partial x}(x,t) = \theta \frac{f_{i+1}^{k+1} - f_i^{k+1}}{\Delta x} + (1-\theta)\frac{f_{i+1}^{k} - f_i^{k}}{\Delta x}, \tag{2.15b}$$

$$\frac{\partial f}{\partial t}(x,t) = \phi \frac{f_{i+1}^{k+1} - f_{i+1}^{k}}{\Delta t} + (1-\phi)\frac{f_i^{k+1} - f_i^{k}}{\Delta t}, \tag{2.15c}$$

where i is the space index, k the time index and $\theta \in [0,1]$, $\phi \in [0,1]$ are weighting coefficients. The generalized Preissmann scheme is depicted in Fig. 2.9.

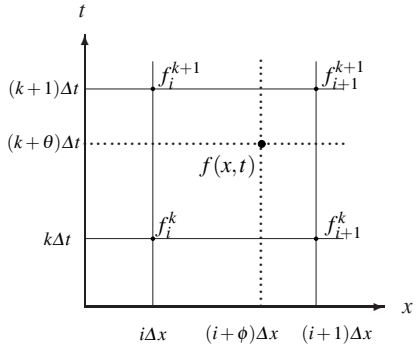

Fig. 2.9 Preissmann implicit discretization scheme

The Preissmann scheme is second-order accurate in both time and space if $\theta = 0.5$ and $\phi = 0.5$, and first-order accurate otherwise. Linear stability analysis shows that the centered scheme ($\phi = 0.5$) is unconditionally stable for $\theta \geq 0.5$. This feature makes it very interesting for practical applications, since contrarily to the case of an explicit scheme, it is not subject to the Courant–Friedrichs–Levy stability condition (2.14) that constrains the time step to small values.

This may explain why the Preissmann scheme has become the standard method for one-dimensional numerical modeling in the field of hydraulic engineering. A stability analysis including convective and friction terms has shown that another condition is necessary for numerical stability in addition to the condition $\theta \geq 0.5$

[16, 22]: the Vedernikov number $\mathscr{V}$ must be smaller than 1, where $\mathscr{V}$ is defined by

$$\mathscr{V} = \frac{a}{b}\frac{A}{R}\frac{\mathrm{d}R}{\mathrm{d}A}F,$$

where a is the exponent on the hydraulic radius and b the exponent on the velocity in the evaluation of the friction slope, A is the cross-sectional area of flow, R the hydraulic radius, and F the Froude number. In the Manning formulation of the friction slope of (2.3), we have $a = \frac{4}{3}$ and $b = 2$.

2.3 Steady Flow Solutions

The steady flow solutions of Saint-Venant equations are obtained by replacing $\frac{\partial}{\partial t}$ by 0 in (2.1) and (2.2). Then, denoting the variables corresponding to the equilibrium regime with a subscript zero ($Q_0(x)$, $Y_0(x)$, etc.), the Saint-Venant equations become:

$$\frac{\mathrm{d}Q_0(x)}{\mathrm{d}x} = 0, \tag{2.16a}$$

$$\frac{\mathrm{d}Y_0(x)}{\mathrm{d}x} = \frac{S_b - S_{f0}(x)}{1 - F_0(x)^2}. \tag{2.16b}$$

F_0 is the Froude number $F_0 = \frac{V_0}{C_0}$ with $C_0 = \sqrt{g\frac{A_0}{T_0}}$, $V_0 = \frac{Q_0}{A_0}$, and T_0 is the top width.

These two equations define an equilibrium regime given by $Q_0(x) = Q_0 = Q_L$ and $Y_0(x)$ solution of the ordinary differential equation (2.16b), for a boundary condition in terms of downstream elevation.

When the right-hand side of (2.16b) is equal to zero, the water depth is constant along the channel. In this case, given $Q_0(x) = Q_0$, the equilibrium solution $Y_0(x) = Y_n$ (also called *normal depth*) can be deduced by solving the following algebraic equation:

$$S_f(Q_0, Y_n) = S_b. \tag{2.17}$$

This specific solution corresponds to the *uniform flow regime*. Equation (2.17) is usually solved numerically with a fixed-point or Newton–Raphson method.

In some cases, the uniform depth can be computed analytically. For large rectangular channels, the hydraulic radius R can be approximated by the water depth Y, and the Manning equation (2.3) reduces to:

$$S_f = \frac{Q^2 n^2}{T^2 Y^{10/3}}. \tag{2.18}$$

Combining (2.17) and (2.18) give the uniform depth Y_n corresponding to a discharge Q_0 in the large rectangular case:

$$Y_n = \left(\frac{Q_0^2 n^2}{T^2 S_b}\right)^{3/10}. \tag{2.19}$$

The uniform flow regime will be specifically developed in the book as an example, since this regime leads to closed-form analytical solutions for the transfer matrix (see Chap. 3). However, we will also show that this specific flow regime is not qualitatively different from realistic nonuniform flow regimes.

Example 2.1. Throughout the book, we will illustrate our results on two trapezoidal prismatic channels, with different characteristics (see Fig. 2.10).

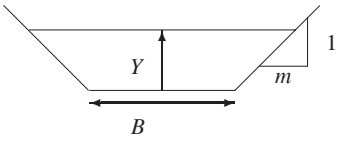

Fig. 2.10 Section of a trapezoidal canal

The channel characteristics are given in Table 2.1, where L is the channel length (m), m the bank slope, B the bed width (m), S_b the bed slope (m/m), n the Manning coefficient ($\mathrm{m}^{-1/3}\mathrm{s}$), and Y_n the normal depth (m) corresponding to the discharge $Q_{\max}$ ($\mathrm{m}^3\mathrm{s}^{-1}$). Canal 1 is a short oscillating canal and canal 2 is a long delayed canal.

Table 2.1 Parameters for the two canals

	L	m	B	S_b	n	Y_n	$Q_{\max}$
Canal 1	3000	1.5	7	0.0001	0.02	2.12	14
Canal 2	6000	1.5	8	0.0008	0.02	2.92	80

Keeping a constant discharge, we compare the backwater curves obtained for different downstream boundary conditions $Y_0(L) = Y_n \times [0.8, 1, 1.2]$ (see Fig. 2.11). We have two types of backwater curves: if $Y_0(L) > Y_n$, then the flow is decelerating along x, this is a so-called "M1" curve (see [20]), and if $Y_0(L) < Y_n$, then the flow is accelerating along x, this is an "M2" curve. The M1 curves are the most widely observed in practice, since they may occur upstream of any kind of obstacle in the flow (hydraulic structure, gate, weir, bridge, etc.). The M2 type curves are observed when there is a sudden drop in the canal or a steep slope downstream.

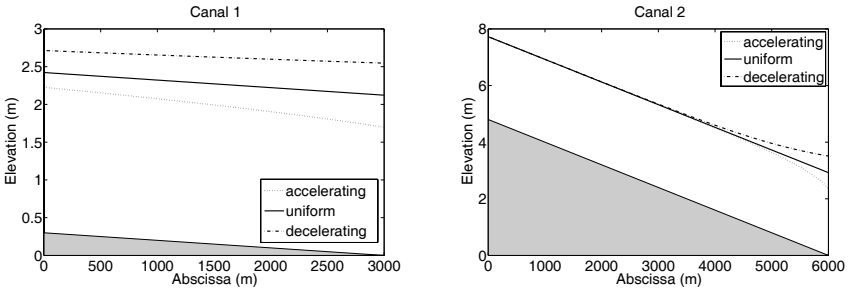

Fig. 2.11 Backwater curves for canals 1 and 2, and various downstream boundary conditions $Y_0(L)$

2.4 Linearized Saint-Venant Equations

We now study the linearized equations around a given steady-state. This is restrictive, since it cannot capture dynamic features such as shocks. Nonetheless, this enables us to use the powerful tools developed for linear systems and, as we will show in Chap. 3, it provides a very detailed analysis of open channel dynamics.

2.4.1 Derivation of the Linearized Equations

The Saint-Venant equations are linearized around an equilibrium steady-state defined by $(Q_0(x), Y_0(x))$. The linearized equations are obtained by putting $Q(x,t) = Q_0(x) + q(x,t)$ and $Y(x,t) = Y_0(x) + y(x,t)$ into (2.1) and (2.2) and expanding in series.

For a given term $f(Q,Y)$ of the Saint-Venant equations, its Taylor expansion can be written as:

$$f(Q,Y) - f(Q_0,Y_0) = f_Q(Q_0,Y_0)q(x,t) + f_Y(Q_0,Y_0)y(x,t) + \text{HOT} \qquad (2.20)$$

where f_Q and f_Y are respectively the partial derivative of f with respect to Q and Y, respectively and HOT stands for higher order terms.

Since we are looking for a *linear* approximation, we keep only the linear terms in y and q in the expansion. All quadratic (and higher order) terms are supposed to be negligible in front of linear terms, even if this is false for large deviations from the equilibrium values. Indeed, the linear approximation is only valid for small deviations from the equilibrium values.

Equation (2.1) then gives:

$$T_0(x)\frac{\partial y}{\partial t} + \frac{\partial q}{\partial x} = 0.$$

After collecting terms in q, y, $\frac{\partial q}{\partial x}$ and $\frac{\partial y}{\partial x}$, (2.2) is linearized as:

$$\frac{\partial q}{\partial t} + 2V_0\frac{\partial q}{\partial x} + \delta q + (C_0^2 - V_0^2)T_0\frac{\partial y}{\partial x} - \tilde{\gamma} y = 0, \tag{2.21}$$

with

$$\tilde{\gamma} = V_0^2\frac{\mathrm{d}T_0}{\mathrm{d}x} + gT_0\Big(\kappa S_{f0} + S_b - (1+2F_0^2)\frac{\mathrm{d}Y_0}{\mathrm{d}x}\Big), \tag{2.22}$$

$$\delta = \frac{2g}{V_0}\Big(S_{f0} - F_0^2\frac{\mathrm{d}Y_0}{\mathrm{d}x}\Big), \tag{2.23}$$

$$\kappa = \frac{7}{3} - \frac{4A_0}{3T_0P_0}\frac{\partial P_0}{\partial Y}, \tag{2.24}$$

and $F_0^2 = \frac{V_0^2 T_0}{gA_0}$ is the Froude number for the equilibrium regime. Dependence on x is omitted for readability.

The model is obtained by linearization around an equilibrium regime defined by (2.16b). Therefore, substituting the expression of S_{f0} obtained from (2.16b) into (2.22) and (2.23), leads to

$$\tilde{\gamma} = V_0^2\frac{\mathrm{d}T_0}{\mathrm{d}x} + gT_0\Big[(1+\kappa)S_b - (1+\kappa-(\kappa-2)F_0^2)\frac{\mathrm{d}Y_0}{\mathrm{d}x}\Big],$$
$$\delta = \frac{2g}{V_0}\Big(S_b - \frac{\mathrm{d}Y_0}{\mathrm{d}x}\Big).$$

The linearized model of open channel flow is therefore given by the two linear partial differential equations:

$$T_0\frac{\partial y}{\partial t} + \frac{\partial q}{\partial x} = 0, \tag{2.25a}$$

$$\frac{\partial q}{\partial t} + 2V_0\frac{\partial q}{\partial x} + (C_0^2 - V_0^2)T_0\frac{\partial y}{\partial x} + \delta q - \tilde{\gamma} y = 0. \tag{2.25b}$$

The initial condition and the boundary conditions are given by:

$$q(x,0) = q_0(x), \quad y(x,0) = y_0(x), \tag{2.26a}$$

$$q(0,t) = u_1(t), \quad q(L,t) = u_2(t). \tag{2.26b}$$

We also assume that the water level deviations are measured at each boundary: $y(0,t)$ and $y(L,t)$.

One may show that with such initial and boundary conditions, the linearized equations are well-posed and satisfy some mathematical properties (see Appendix E for details).

To simplify the notations and to facilitate the forthcoming mathematical analysis, we will use an alternative expression for the linearized Saint-Venant equations, by defining $a(x,t) = T_0(x)y(x,t)$, and expressing the equations as a function of $q(x,t)$

and $a(x,t)$. We also define

$$\begin{aligned}\alpha(x) &= C_0(x) + V_0(x)\\ \beta(x) &= C_0(x) - V_0(x)\\ \gamma(x) &= \frac{1}{T_0(x)}\Big(\tilde{\gamma}(x) + (C_0^2(x) - V_0^2(x))\frac{\mathrm{d}T_0}{\mathrm{d}x}(x)\Big).\end{aligned}$$

The linearized equations are then given by:

$$\frac{\partial a}{\partial t} + \frac{\partial q}{\partial x} = 0, \tag{2.27a}$$

$$\frac{\partial q}{\partial t} + (\alpha - \beta)\frac{\partial q}{\partial x} + \alpha\beta\frac{\partial a}{\partial x} + \delta q - \gamma a = 0, \tag{2.27b}$$

with

$$\gamma = \frac{C_0^2}{T_0}\frac{\mathrm{d}T_0}{\mathrm{d}x} + g\Big[(1+\kappa)S_b - (1+\kappa-(\kappa-2)F_0^2)\frac{\mathrm{d}Y_0}{\mathrm{d}x}\Big].$$

Equations (2.27a–2.27b) are simpler for the mathematical analysis, and are equivalent to (2.25a–2.25b). The solution in terms of variations of water level $y(x,t)$ can readily be deduced by dividing by $T_0(x)$ the solution obtained in terms of variations of wetted area $a(x,t) = T_0(x)y(x,t)$.

Finally, we can rewrite the linearized Saint-Venant equations as follows:

$$\frac{\partial \xi}{\partial t} + \mathbf{A}(x)\frac{\partial \xi}{\partial x} + \mathbf{B}(x)\xi = 0, \tag{2.28}$$

where $\xi(x,t) = (a(x,t), q(x,t))^T : [0,L]\times[0,+\infty) \to \Omega \in \mathbb{R}^2$ is the state of the system and $\mathbf{A}(x) = \begin{pmatrix} 0 & 1 \\ \alpha(x)\beta(x) & \alpha(x)-\beta(x)\end{pmatrix}$, $\mathbf{B}(x) = \begin{pmatrix} 0 & 0 \\ -\gamma(x) & \delta(x)\end{pmatrix}$.

Example 2.2 (Parameters of the linearized Saint-Venant equations for the example canals). Table 2.2 gives the parameters of the example canals at uniform flow.

Table 2.2 Parameters for the two canals at uniform flow

	L	α	β	γ	δ	T_0
Canal 1	3000	4.63	3.33	0.0027	0.003	13.37
Canal 2	6000	6.81	2.39	0.0218	0.0071	16.77

Let us note that the linearized Saint-Venant equations are hyperbolic equations, since the eigenvalues of matrix $\mathbf{A}$, namely $\alpha(x)$ and $-\beta(x)$, are real. In the subcritical flow case, the eigenvalues are of opposite sign.

2.4.2 Characteristic Form

Let us introduce the following change of variable, which corresponds to the characteristic form of the linearized equations:

$$\chi_1(x,t) = q(x,t) + \beta(x)T_0(x)y(x,t), \tag{2.29a}$$
$$\chi_2(x,t) = q(x,t) - \alpha(x)T_0(x)y(x,t). \tag{2.29b}$$

The inverse transform is given by:

$$y(x,t) = \frac{1}{T_0(\alpha+\beta)}[\chi_1(x,t) - \chi_2(x,t)], \tag{2.30a}$$
$$q(x,t) = \frac{1}{\alpha+\beta}[\alpha\chi_1(x,t) + \beta\chi_2(x,t)]. \tag{2.30b}$$

Using a matrix notation and the fact that $\xi = (T_0 y, q)^T$, we have:

$$\chi(x,t) = \mathbf{X}(x)\xi(x,t),$$

with $\mathbf{X}(x) = \begin{pmatrix} \beta(x) & 1 \\ -\alpha(x) & 1 \end{pmatrix}$.

This change of variable enables us to diagonalize matrix $\mathbf{A}(x)$ as follows:

$$\mathbf{A}(x) = \mathbf{X}(x)^{-1}\mathbf{D}(x)\mathbf{X}(x),$$

with

$$\mathbf{D}(x) = \begin{pmatrix} \alpha(x) & 0 \\ 0 & -\beta(x) \end{pmatrix},$$

and

$$\mathbf{X}(x)^{-1} = \frac{1}{\alpha(x)+\beta(x)} \begin{pmatrix} 1 & -1 \\ \alpha(x) & \beta(x) \end{pmatrix}.$$

Equation (2.28) can then be rewritten as:

$$\frac{\partial \chi}{\partial t} + \mathbf{D}(x)\frac{\partial \chi}{\partial x} + \mathbf{E}(x)\chi = 0, \tag{2.31}$$

with $\mathbf{E}(x) = [\mathbf{X}(x)\mathbf{B}(x) - \mathbf{D}(x)\mathbf{X}'(x)]\mathbf{X}(x)^{-1}$, where $f'(x)$ denotes the derivative of f with respect to x.

This change of variable corresponds to the characteristic form of the equations. Indeed, the new variable $\chi(x,t)$ verifies:

$$\frac{\mathrm{d}\chi_1}{\mathrm{d}t}(x_1,t) = -e_{11}(x_1)\chi_1(x_1,t) - e_{12}(x_1)\chi_2(x_1,t), \tag{2.32a}$$

$$\frac{\mathrm{d}x_1}{\mathrm{d}t} = \alpha(x_1), \tag{2.32b}$$

$$\frac{\mathrm{d}\chi_2}{\mathrm{d}t}(x_2,t) = -e_{21}(x_2)\chi_1(x_2,t) - e_{22}(x_2)\chi_2(x_2,t), \tag{2.32c}$$

$$\frac{\mathrm{d}x_2}{\mathrm{d}t} = -\beta(x_2), \tag{2.32d}$$

with $\mathbf{E}(x) = (e_{ij}(x))$ defined by:

$$e_{11} = \frac{1}{\alpha+\beta}\Big[-\gamma+\alpha\delta-\alpha\beta'\Big], \tag{2.33a}$$

$$e_{12} = \frac{1}{\alpha+\beta}\Big[\gamma+\beta\delta+\alpha\beta'\Big], \tag{2.33b}$$

$$e_{21} = \frac{1}{\alpha+\beta}\Big[-\gamma+\alpha\delta-\beta\alpha'\Big], \tag{2.33c}$$

$$e_{22} = \frac{1}{\alpha+\beta}\Big[\gamma+\beta\delta+\beta\alpha'\Big], \tag{2.33d}$$

where we have dropped the argument x for readability, and α' and β' denote the derivatives of α and β with respect to x.

This change of variable leads to the characteristic form of the linearized Saint-Venant equations. Indeed, one may show that the variables $\chi_1(x,t)$ and $\chi_2(x,t)$ are closely linked to the characteristic variables $j_1(x,t) = v(x,t)+2c(x,t)$ and $j_2(x,t) = v(x,t)-2c(x,t)$, which are the deviations from the characteristic variables J_1 and J_2 around the reference steady flow. To this end, we express $\chi_1(x,t)$ and $\chi_2(x,t)$ in terms of $v(x,t)$ and $c(x,t)$, the variations of velocity and celerity from the steady flow values $V_0(x)$ and $C_0(x)$. Such a link is especially simple in the case of a rectangular channel. Indeed, in that case, we have $v = \frac{q}{T_0Y_0} - \frac{V_0}{Y_0}y$ and $c = \frac{C_0}{2Y_0}y$, which gives in turn:

$$y = \frac{2Y_0}{C_0}c,$$
$$q = T_0Y_0\Big(v+2\frac{V_0}{C_0}c\Big).$$

Substituting this into the expressions of $\chi(x,t)$ yields:

$$\chi_1 = q+(C_0-V_0)T_0y = T_0Y_0(v+2c),$$
$$\chi_2 = q-(C_0+V_0)T_0y = T_0Y_0(v-2c).$$

Therefore the variables $\chi_1(x,t)$ and $\chi_2(x,t)$ are proportional to the characteristics variables $j_1(x,t)$ and $j_2(x,t)$.

Remark 2.1 (Riemann coordinates in nonuniform flow). From the expression of matrix $\mathbf{E}(x)$, we see that even in the case where the friction and the slope can be neglected ($\delta(x) \approx 0$ and $\gamma(x) \approx 0$), but when the flow is not uniform (e.g., because of a nonuniform geometry), the Riemann coordinates are no longer invariants. This also appears in the general characteristic form, with a supplementary term on the right-hand side due to the nonprismatic geometry.

We now consider simplified models obtained from the Saint-Venant equations.

2.5 Approximate Hydraulic Models for Flow Routing

The Saint-Venant equations require a lot of data (geometry of the channel, longitudinal profile, roughness coefficient) that are not always available in the case of rivers. There are also cases where some terms can be neglected in the equations, leading to simplified models of open channel flow.

2.5.1 The Diffusive Wave

Assuming the inertia terms ($\frac{\partial Q}{\partial t} + \frac{\partial Q^2/A}{\partial x}$) are negligible with respect to ($Ag\frac{\partial z}{\partial x}$), the water elevation $z = Y + S_b x$ can be eliminated from the Saint-Venant equations (2.1) and (2.2), leading to the diffusive wave equation [12]:

$$\frac{\partial Q}{\partial t} + C(Q,z,x)\frac{\partial Q}{\partial x} - D(Q,z,x)\frac{\partial^2 Q}{\partial x^2} = 0, \tag{2.34}$$

with $Q(x,t)$ the discharge (m^3/s), $C(Q,z,x)$ the celerity (m/s), and $D(Q,z,x)$ the diffusion (m^2/s).

C and D are given by the following formulas:

$$C(Q,z,x) = \frac{1}{T^2\frac{\partial S_f}{\partial Q}}\left[\frac{\partial T}{\partial x} - \frac{\partial (TS_f)}{\partial z}\right], \tag{2.35}$$

$$D(Q,z,x) = \frac{1}{T\frac{\partial S_f}{\partial Q}}, \tag{2.36}$$

where T stands for the water surface top width.

Supposing uniform geometry and uniform flow regime, one may obtain analytical expressions of C and D in some cases.

With a uniform geometry, (2.35) and (2.36) give $C = 5Q/(3A)$ and $D = Q/(2TS_b)$, where S_b stands for the bed slope of the reach.

In the case of a large rectangular channel, the normal depth is much lower than the surface width $Y \ll T$. The hydraulic radius can be approximated by the normal depth $R \simeq Y$. Manning Strickler equation (2.3) then reads:

$$Q = KA\sqrt{S_b}Y^{2/3}.$$

As $A = TY$, one gets an explicit expression for Y:

$$Y = \left(\frac{Q}{KT\sqrt{S_b}}\right)^{3/5}.$$

C and D can then be expressed as functions of the discharge Q:

$$C = \frac{5K^{3/5}S_b^{3/10}}{3T^{2/5}}Q^{2/5},$$
$$D = \frac{Q}{2TS_b}.$$

Using the variables $\Theta = 1/(3.6C)$ (hydraulic time-lag expressed in h/km) and $Z = 250C/D$ (hydraulic diffusion expressed in km^{-1}) one gets:

$$\Theta = \alpha_\Theta Q^{\beta_\Theta},$$
$$Z = \alpha_Z Q^{\beta_Z},$$

with $\alpha_\Theta = 6T^{-0.4}K^{0.6}S_b^{0.3}$, $\beta_\Theta = -0.4$, $\alpha_Z = 625/3K^{0.6}T^{0.6}S_b^{1.3}$, $\beta_Z = -0.6$.

2.5.2 The Hayami Model

The linear equation obtained with the hypothesis that C and D are constant is called the Hayami equation. This linear hypothesis is valid when the discharge stays within a limited range of variation.

The Hayami equation is a linear partial derivative equation representing the discharge transfer in a river reach around an equilibrium point:

$$\frac{\partial q}{\partial t} + C\frac{\partial q}{\partial x} - D\frac{\partial^2 q}{\partial x^2} = 0, \tag{2.37}$$

where

- q is the discharge (m^3/s,
- C the celerity coefficient (m/s), and
- D the diffusion coefficient (m^2/s).

This parabolic partial differential equation is closely related to the heat equation, which can be controlled using backstepping-type methods [10].

2.6 Summary

In this chapter, we have derived the Saint-Venant equations, which are the classical distributed parameter model for one-dimensional open channel flow. These equations are based on a series of assumptions that proved to be very efficient for describing flow in rivers, canals, and sewers. The equations can be put in the characteristic form, which is useful for understanding the underlying physical phenomenon described by the equations.

We then derived a linearized Saint-Venant model, valid for small variations around an equilibrium flow regime. This model consists of two linear partial differential equations, which will be analyzed in detail and used as a basis for controller design in the following. In fact, it would be desirable to be able to use the nonlinear Saint-Venant equations to design automatic controllers, but this is a very difficult problem, and remains open at the moment. Some preliminary results have been obtained for the horizontal frictionless case using Riemann invariants [9], but much more needs to be done to be able to stabilize the full nonlinear Saint-Venant equations.

The linearized equations are derived around a nonuniform steady flow regime, following the approach developed in [17, 11].

The mathematical analysis of the linearized equations is performed in Appendix E.

References

[1] Abbott M (1966) An introduction to the method of characteristics. Elsevier, New York
[2] Abbott MB (1979) Computational hydraulics. Elements of the theory of free surface flows. Pitman Publishing, London, 324 p
[3] Bardos C, Le Roux A, Nedelec J (1979) First order quasilinear equations with boundary conditions. Commun in Part Diff Eqs 4(9):1017–1034
[4] Boussinesq VJ (1877) Essai sur la théorie des eaux courantes, vol 23. Mémoires présentés par divers savants à l'Académie des Sciences, Paris
[5] Chow V (1988) Open-channel hydraulics. McGraw-Hill, New York, 680 p
[6] Cunge J, Holly F, Verwey A (1980) Practical aspects of computational river hydraulics. Pitman Advanced Publishing Program
[7] Evans L (1998) Partial differential equations, Graduate studies in mathematics, vol 19. American Mathematical Society, Providence, RI
[8] Favre H (1935) Etude théorique et expérimentale des ondes de translation dans les canaux découverts. Dunod, Paris
[9] de Halleux J, Prieur C, Coron JM, d'Andréa Novel B, Bastin G (2003) Boundary feedback control in networks of open-channels. Automatica 39:1365–1376
[10] Krstic M, Smyshlyaev A (2008) Boundary control of PDEs: A course on backstepping designs. SIAM
[11] Litrico X, Fromion V (2004) Frequency modeling of open channel flow. J Hydraul Eng 130(8):806–815
[12] Miller W, Cunge J (1975) Simplified equations of unsteady flow, in Mahmood K, Yevjevich V (eds.), *Unsteady flow in open channels*. Water Resources Publications, Fort Collins, CO, pp 183–257

[13] Mohapatra PK, Chaudhry MH (2004) Numerical solution of Boussinesq equations to simulate dam-break flows. J Hydraul Eng 130(2):156–159
[14] Preissmann A (1961) Propagation des intumescences dans les canaux et rivières. In: 1er Congrès de l'Association Française de Calcul, Grenoble, France, pp 433–442
[15] Barré de Saint-Venant A (1871) Théorie du mouvement non-permanent des eaux avec application aux crues des rivières et à l'introduction des marées dans leur lit. Comptes rendus Acad Sci Paris 73:148–154, 237–240
[16] Samuels P, Skeels C (1990) Stability limits for Preissmann's scheme. J Hydraul Eng 116(8):997–1012
[17] Schuurmans J (1997) Control of water levels in open-channels. PhD thesis, ISBN 90-9010995-1, Delft University of Technology
[18] Soares-Frazao S, Zech Y (2002) Undular bores and secondary waves - experiments and hybrid finite-volume modelling. J Hydr Res 40(1):33–43
[19] Strub I, Bayen A (2006) Weak formulation of the boundary condition for scalar conservation laws: an application to highway traffic modelling. Int J Robust Nonlin Contr 16(16):733–748
[20] Sturm T (2001) Open-channel hydraulics. McGraw-Hill, New York
[21] Treske A (1994) Undular bores (Favre waves) in open channels – experimental studies. J Hydr Res 32(3):355–370
[22] Venutelli M (2002) Stability and accuracy of weighted four-point implicit finite difference schemes for open channel flow. J Hydraul Eng 128(3):281–288

http://www.springer.com/978-1-84882-623-6

Modeling and Control of Hydrosystems

Litrico, X.; Fromion, V.

2009, XV, 409 p. With online files/update., Hardcover
ISBN: 978-1-84882-623-6